

Bonding of Endohedral Atoms in Small Carbon Fullerenes

Koblar Jackson*

Department of Physics, Central Michigan University, Mt. Pleasant, Michigan 48859

Efthimios Kaxiras

Department of Physics and Division of Applied Sciences, Harvard University, Cambridge, Massachusetts 02138

Mark R. Pederson

Complex Systems Theory Branch, Naval Research Laboratory, Washington, D.C. 20375

Received: December 9, 1993; In Final Form: April 27, 1994*

We present a simple model for understanding the bonding of endohedral atoms in small fullerene cages, based on their approximate spherical shape. Previous work has shown that the one-electron wave functions of a fullerene cage can be assigned angular momentum quantum numbers which describe their overall angular character. These quantum numbers form the basis for approximate selection rules which govern the bonding with endohedral atoms. With this model we successfully address the very different bonding of various tetravalent elements in C_{28} and the remarkably strong bonding of U in this small fullerene. We also make several specific predictions regarding the stability of other endohedral complexes.

Introduction

The fullerenes,¹ closed, spheroidal shells of 3-fold coordinated carbon atoms, have now been isolated in a number of forms, including the original single-shell cages, and the more recent single- and multiple-shell tubes^{2,3} and the nested-cage "onions".⁴ The ability of these carbon cages to encapsulate other atoms was first demonstrated for the prototypical fullerene C_{60} .⁵ Such systems, dubbed "endohedral complexes" and denoted by $M@C_n$, present the possibility of making stable cages with tailored electronic properties. Compounds of this type may lead to novel ferroelectrics⁶ and superconducting materials⁷ and possibly to even more exotic electrical, chemical, and biological applications.

Experiments⁸ have recently been reported on the endohedral complexes of C_{28} ⁹ which can trap uranium atoms producing a remarkably stable $U@C_{28}$ molecule. Hf, Zr, and Ti also appear to form stable endohedral complexes with C_{28} . Since each of these endohedral atoms forms chemical compounds with a valence state of 4^+ , it has been speculated⁸ that C_{28} is a tetravalent cluster. Theoretical work^{8,10–12} lends support to this conjecture, showing that the C_{28} cluster has an open-shell electronic structure consisting of four nearly degenerate orbitals at the Fermi level (a singlet and a triplet). These states are four electrons short from being completely filled. Quantum mechanical calculations based on density functional theory confirm that for some tetravalent atoms, M, the $M@C_{28}$ compounds have large binding energies, for example, 12.6 eV for $M = Zr^{10}$ and 11.8 eV for $M = Ti$.¹¹ This is much stronger than binding energies of $M@C_{60}$ complexes, which typically lie in the range 1–2 eV. On the other hand, several other compounds of tetravalent atoms inside C_{28} were shown to be marginally stable or even unstable.¹²

To understand the bonding of atoms inside small fullerene cages, we recently conducted a systematic study of the tetravalent group IV endohedral atoms (C to Sn) in C_{28} .¹² These elements span a broad range of atomic sizes. Surprisingly, we found very little bonding between any of the group IV endohedrals and C_{28} . For example, Si and Ge have binding energies 1.3 and 0.9 eV, whereas C and Sn are *not bound* (binding energies of -0.1 and -0.4 eV). The vast difference in the binding energy of Zr on the one hand and Sn on the other, even though both are tetravalent

metals, indicates that the cluster–atom interaction in these two cases is very different. In this paper we examine the character of the electronic states of the cluster and show that the approximate spherical shape of the cage has a profound influence on the bonding to endohedral atoms. Our theoretical analysis provides a concise understanding of the differences between the various endohedrals in C_{28} and affords specific predictions on the type of atom that will lead to optimally stable complexes. On the basis of this analysis, we also comment on the remarkable stability of the $U@C_{28}$ complex. Direct, first-principles calculations for this system are very demanding,¹³ due to the open f-shell of the U atom and the need to treat the U core electrons relativistically.

Electronic States of C_{28}

The electronic states of the C_{28} cluster were determined using state-of-the-art quantum mechanical calculations based on the Hohenberg–Kohn–Sham local (spin) density approximation (LDA).¹⁴ We employ a basis set of Gaussian-type orbitals and a numerical integration scheme¹⁵ to obtain high accuracy in computing the cluster total energy. The forces on the atoms are computed using the Hellmann–Feynman–Pulay approach.¹⁶ Geometry optimization is performed by combining the total energy and the forces in a conjugate gradient algorithm. The relaxed structure for C_{28} calculated within this scheme is shown in Figure 1. This structure has some similarities with, but also some important differences from C_{60} . Both structures consist of pentagonal and hexagonal rings of 3-fold-coordinated carbon atoms, spread over an approximately spherical shell. In C_{60} the 12 pentagons do not share any corners or edges. This produces a more spherical shape, since pentagons are loci of high curvature. By contrast, in C_{28} the 12 pentagons are grouped in four triplets. Each pentagon shares a common apex corner and two edges with the two other pentagons of the same triplet. This arrangement produces a less spherical shape, with the four apex corners being the points of highest curvature. For reference we compare some of the calculated properties of C_{28} and C_{60} ¹⁷ in Table 1. The calculated eigenvalue spectrum for C_{28} appears in Figure 2.

As seen in Figure 1, while the full symmetry of C_{28} is tetrahedral (T_d),⁹ its overall shape remains approximately spherical. A number of papers¹⁸ have pointed out the strong influence of the nearly spherical shape of C_{60} on the character of its valence electron

* Abstract published in *Advance ACS Abstracts*, July 15, 1994.

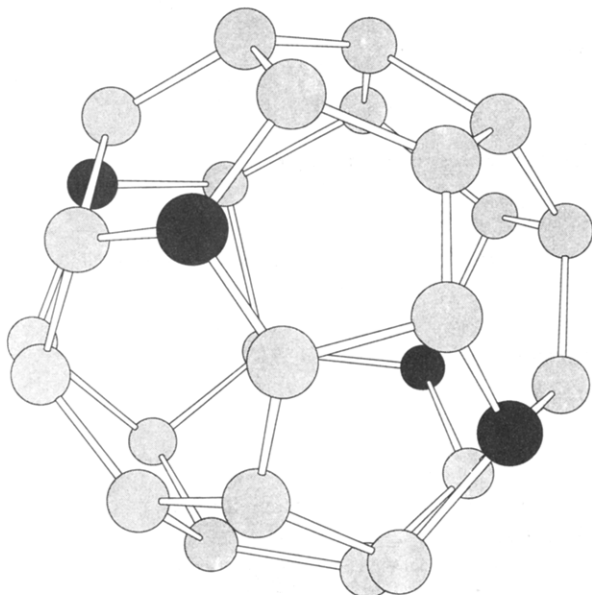


Figure 1. Structure of the C_{28} fullerene cluster. The four shaded atoms define the plane used to plot wave functions in Figure 3.

TABLE 1: Comparison of Selected Properties of C_{28} and C_{60} ^a

	C_{28}	C_{32}	C_{60}
$\langle r \rangle$ (au)	4.57	4.90	6.61
E_B (eV)	8.05	8.22	8.54
I (eV)	7.92	8.40	7.61
A (eV)	3.83	3.02	2.75
HOMO–LUMO gap (eV)	0.00	1.20	1.74

^a $\langle r \rangle$ is the average radius of the fullerene cage, E_B is the binding energy per atom calculated within the LDA, I is the ionization energy of the cluster, and A the electron affinity. The HOMO–LUMO gap is also given. In the case of C_{28} the HOMO is partially occupied, so strictly speaking the occupied and unoccupied states are NOT separated by an energy gap.

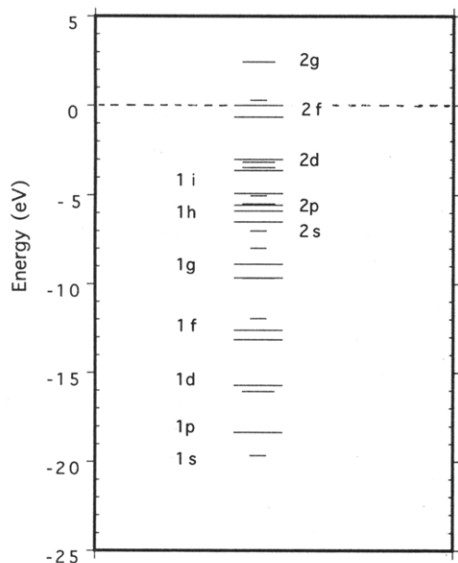


Figure 2. One-electron LDA eigenvalue spectrum of C_{28} . The length of the lines represents the degeneracy (1, 2, or 3) of the energy levels. The labels indicate principal and angular momentum quantum numbers for the cluster eigenstates as discussed in the text.

states. The argument is essentially that, to first approximation, the potential energy surface seen by the valence electrons in C_{60} is spherical, so that the valence electron states have an angular character that is approximately that of angular momentum eigenstates, and thus can be labeled by an orbital quantum number l . In addition, the valence states can be assigned a second quantum

number reflecting the *radial* character of the wave functions. The carbon atoms on a fullerene cage are approximately sp^2 hybridized, with the hybrid orbitals forming σ bonds to other atoms. The fourth orbital has mainly p_z character and is directed radially outward from the cluster center. Where possible, these orbitals take part in π bonds on the surface. The cluster states corresponding to the lower energy σ bonds have no radial node, while the states corresponding to π bonds change sign in going from the interior of the cluster to the exterior.

Although C_{28} is smaller and less spherical than C_{60} , the same analysis can be applied to its valence electron states. In Figure 2 we show the one-electron eigenvalue spectrum for C_{28} , assigning Nl quantum numbers to each state ($N = 1$ for σ states and $N = 2$ for π states). We determined the orbital number l by finding the overlap of each of the cluster wave functions with the spherical harmonics. In each case a given wave function had significant overlap with functions of only a single l . The radial number N was determined both by using the known splittings of the spherical eigenstates due to tetrahedral distortions¹⁹ and by directly plotting the wave functions to determine the presence or absence of radial nodes.

The states straddling the Fermi level of C_{28} are the $Nl = 2f$ states of the cluster. In the spin-unpolarized calculation, the highest occupied molecular orbital (HOMO) is a $2f$ state with t_2 symmetry (3-fold degenerate) and contains four electrons. The lowest unoccupied molecular orbital (LUMO) is a $2f$ state with a_1 symmetry (singly degenerate) lying 0.25 eV above the HOMO. This situation is consistent with a total of 28 electrons available to fill π states, a number sufficient to occupy all the $N = 2$ states through $l = 2$, leaving 10 for the $2f$ ($l = 3$) manifold which can hold a total of 14. The next state in the eigenvalue spectrum of C_{28} above the $2f$ manifold is a $2g$ state, which lies 2.5 eV above the HOMO (see Figure 2).

To better illustrate the nature of the cluster states we show in Figure 3 wave functions corresponding to the $1s$, $2s$, $2p$, and $1g$ states, plotted in a plane containing the four shaded atoms of Figure 1, and cutting through the center of the cluster. The $1s$, $2s$, and $1g$ wave functions all transform in the a_1 representation of the T_d group, while the $2p$ transforms in the t_2 representation. The similarities between the cluster states and the corresponding pure angular momentum states are striking. The s-like cluster wave functions are characterized by a constant sign as a function of azimuthal angle. The $2p$ cluster state, by contrast, has a characteristic p-like nodal plane. The $1g$ function has several nodal planes, as expected for a state of high angular momentum. Comparing the $1s$ and $2s$ cluster wave functions, one clearly sees the existence of the radial node in the $N = 2$ function in going from the center of the cluster outward.

Meta-Atom View of Endohedral Bonding

What emerges from Figures 2 and 3 is a meta-atom picture of the C_{28} cluster: The cluster wave functions share general features with atomic wave functions and thus can be meaningfully labeled by corresponding quantum numbers. This viewpoint can be used to understand cluster properties, and in particular, the bonding of C_{28} to endohedral atoms. Covalent bonding in $M@C_{28}$ is the result of mixing cage states and endohedral atom orbitals in bonding combinations. Symmetry dictates that only orbitals transforming in the same irreducible representation of the point group of the complex (T_d) can be mixed in a given bonding state. However, as discussed above, the C_{28} wave functions have a strong angular momentum character due to the nearly spherical shape of the cluster. Since l is a good quantum number for the endohedral atom orbitals, this implies that wave functions of the endohedral atom and of the cluster labeled by different l will not mix strongly to form eigenstates of the complex, even if they belong to the same T_d irreducible representation. This approximate l -selection rule is the key to endohedral bonding in C_{28} .

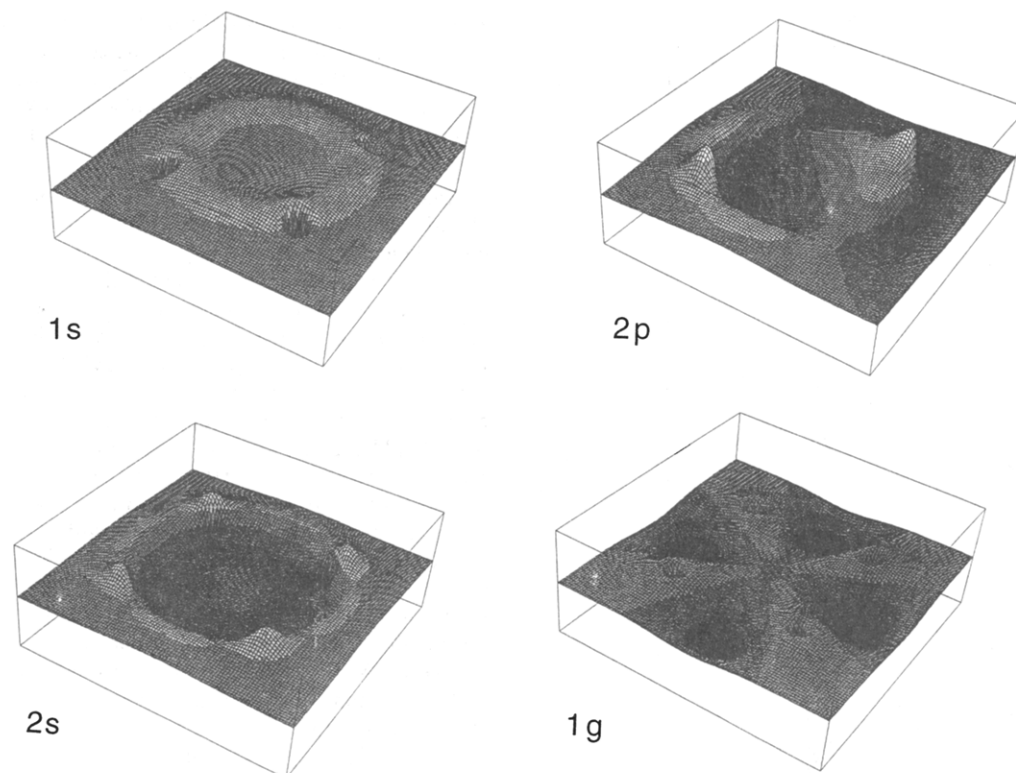


Figure 3. Wave functions of the C_{28} cluster plotted in the plane containing the four shaded atoms in Figure 1. The labels for the wave functions are the principal and angular momentum quantum numbers described in the text. The height z in the figure represents the amplitude of the wave functions over the plane. Lighter shading indicates positive amplitude, and darker shading negative.

To illustrate the point, Figure 4 shows the energy levels of the isolated C_{28} cluster, the free endohedral atom, and the $M@C_{28}$ complex for $M = Sn$ and $M = Zr$. The levels are displayed in correlation diagrams to show the effects of endohedral bonding. A striking feature of the diagrams is that most of the cluster energy levels are unaffected by interactions with the endohedral atoms. In the case of $Sn@C_{28}$, only the 2s and 2p cluster levels are significantly shifted. These levels have the same angular character as the Sn 5s and 5p valence states, in agreement with our l -selection rule. The resulting bonding states have most of their weight in cage orbitals, with a small admixture of Sn orbitals. Conversely, the antibonding states have predominantly Sn character, with a small admixture of cage orbitals. Both antibonding levels lie above the cage HOMO, and, as a result, both the l_2 HOMO and the a_1 LUMO of the empty cage are filled in the complex, opening a gap of 1.2 eV to the antibonding s state, which is the LUMO of the endohedral complex.

In the case of endohedral Zr (valence electron configuration $5s^2 4d^2$), the Zr 4d states form bonding and antibonding combinations with the 2d cage orbitals, leaving the remaining cage levels essentially unaffected. The bonding levels have a predominantly cage-centered 2d character, with a small admixture of endohedral 4d orbitals, and are pushed down considerably relative to the 2d levels of the bare C_{28} . The character of the anti-bonding states is mostly Zr 4d, and these states lie well above the Fermi level of the complex. The Zr 5s orbital also lies well above the Fermi level. The electrons that originally resided in that atomic level are transferred to the lower-lying 2f states of the $Zr@C_{28}$ complex which are now completely filled. This produces a large gap of about 2.3 eV to the LUMO, which is a cluster state of e character with quantum numbers 2g.

Our first-principles calculations show a large difference in the binding energy of $Sn@C_{28}$ and $Zr@C_{28}$: the energy of the $Sn@C_{28}$ complex is 0.35 eV *higher* than that of the isolated cage and Sn atom, while the $Zr@C_{28}$ complex is 12.6 eV *lower* in energy than the isolated cage plus Zr atom. This difference in binding is reflected in the correlation diagrams of Figure 4 and

is related to the depth of the cage 2s and 2p orbitals below the Fermi level (~ 7 eV), compared to that of the cage 2d orbital (~ 3 eV), which makes the former orbitals much less effective for bonding to the endohedral atom. For example, because of the depth of the 2s cage levels, the antibonding s level in $Sn@C_{28}$ falls very near the Fermi level. In effect, the electrons originally occupying the Sn 5s orbital are transferred to states at the Fermi level, which are nearly degenerate with the antibonding level. This offsets the energy gained by the downward shift of the bonding 2s level (Figure 4a). Furthermore, the bonding shift of the 2p level is very small, in part because of the large energy difference between this state and the Sn 5p orbital. In the $Zr@C_{28}$ complex, the Zr4d orbitals interact strongly with the cage 2d, leading to large bonding/antibonding shifts. In this case, all the antibonding states are well above the Fermi level, so that the complex derives strong net bonding from the covalent interaction between the d orbitals of the cluster and the endohedral atom (Figure 4b).

U@C₂₈ and Beyond

The meta-atom model of endohedral bonding developed above provides direct insight into the remarkable stability of the $U@C_{28}$ complex. U has a valence electron configuration $7s^2 6d^1 5f^3$. The U 5f orbitals can be expected to bond strongly with the 2f states of C_{28} which straddle the Fermi level of the cluster (they are partially filled in the empty cage). The character of the bonding levels is expected to be mostly cage-like, with some admixture of U 5f orbitals. Due to the mixing, the resulting bonding levels of the complex will be shifted down in energy compared to the 2f levels of C_{28} . Conversely, the f antibonding levels will have a predominant U 5f character, and will lie above the Fermi level of the empty cage. Electron counting shows that the bonding levels will be completely filled, with two of the U valence electrons remaining to go into the next unoccupied level. The character of this level will depend on the details of the bonding in $U@C_{28}$. The fact that $U@C_{28}$ appears to be chemically stable⁸ suggests either that the complex has a completely filled HOMO and a significant HOMO–LUMO gap, or that the complex has a

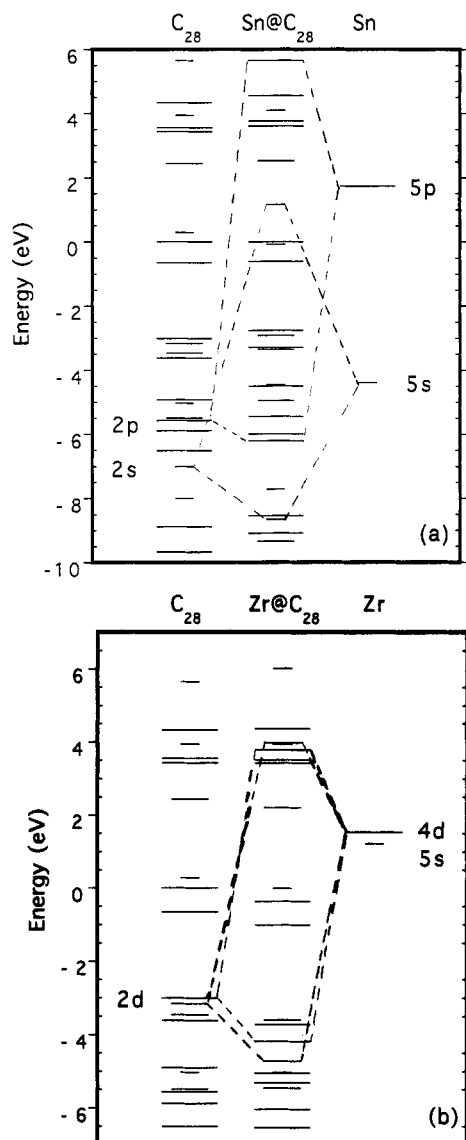


Figure 4. Correlation diagram indicating energy level shifts due to endohedral bonding for the $\text{Sn}@C_{28}$ and $\text{Zr}@C_{28}$ complexes.

partially filled HOMO that is centered mainly on the U atom and is physically shielded from reactant molecules by the cage. Possible electronic configurations consistent with these arguments include a filled U 7s state as the HOMO or a (weakly) antibonding d or f state as the HOMO. Additional bonding for the complex is likely to come through the interaction of the U 6d states with the cage 2d states, in a manner similar to that in $\text{Zr}@C_{28}$. The combined result of the f and d orbital mixing would produce very strong bonding between U and the C_{28} cage.

Our model can be used to make predictions regarding the bonding of endohedral atoms in C_{28} that have not been tried experimentally. In general, the analysis given above suggests that only atoms with valence electrons of angular momentum d or f are good candidates for strong bonding inside C_{28} . Atoms with valence electrons of angular momentum s and p will be forced to interact with cluster states well below the Fermi level (as in the case of $\text{Sn}@C_{28}$ discussed earlier), which does not lead to strong bonding. With this constraint, we consider separately the likely candidates in the periodic table which would interact with the cage mostly through their d valence states (transition metals) and those that will interact mostly through their f valence states (rare earth metals). In making our predictions, we also take into account the known oxidation states of the elements. We expect this to be a relevant consideration, because the bonding states of the endohedral complexes are mostly cage-like, implying

a degree of charge transfer from the vicinity of the atom to the cage. Since four electrons are needed to fill the bonding combinations of the 2f states of the C_{28} cage, we suggest that the optimal oxidation state for an endohedral is 4^+ . All the stable complexes observed thus far (Ti , Zr , Hf , and $\text{U}@C_{28}$) consist of elements that fall into this category.

Among the transition metals, Ti , Zr , and Hf (which have already been shown to produce stable complexes: see ref 8), are ideal choices according to our theory. The valence d states of these endohedral atoms will bond to the 2d levels of the cage as discussed above for Zr . These atoms also possess four valence electrons which will exactly fill all the available states below the Fermi level in the $\text{M}@C_{28}$ complex leaving a stable, closed-shell system. Atoms with fewer valence electrons, e.g., Se , Y and La , cannot fill all the available states at the Fermi level, so that while they should experience some bonding to the cage, the resulting systems should be less chemically stable than the group IVB endohedrals. Atoms with more valence electrons will also experience less net bonding since the additional electrons will be forced into higher lying levels, producing in general a less stable compound. Possible exceptions are cases in which the surplus electrons completely fill the higher-lying levels *without* disturbing the bonding (i.e., they are not antibonding states). In such cases, a large HOMO-LUMO gap for the complex may be produced, making the complex chemically stable. Interesting possibilities include atoms that have an even number of surplus valence electrons in low angular momentum states. In these cases, the *l*-selection rule will cause the surplus electrons to lie in nonbonding states close to the Fermi level of the empty cage. The following elements seem particularly promising in this context: Mo and W , with six valence electrons, and Ru and Os , with eight valence electrons. All of these elements exist in a 4^+ oxidation state. The surplus electrons could fill an s-like atomic state (for the hexavalent endohedrals) or the next available cage state which has e character and quantum numbers 2g and can accommodate four electrons (for the octavalent endohedrals).

Among the f electron atoms, U is probably the ideal case, possessing four electrons that can fill the f bonding levels of the complex, and two nonbonding electrons. Nd has an electronic structure similar to U and should therefore also be very strongly bound in C_{28} . One caveat is that Nd exists only in a 3^+ oxidation state, which indicates its reluctance to form bonds by sharing more than three valence electrons. Atoms with one fewer valence electron, i.e., Pr, and Pa, will have an open-shell electronic configuration, which may make the endohedral complexes of these atoms chemically less stable. Th and Ce have two fewer valence electrons than U and thus should give closed-shell endohedral complexes with a binding energy possibly comparable to that of Zr. Both of these elements exist in a 4^+ oxidation state. Atoms to the right of U and Nd in the periodic table are likely to show less binding with C_{28} , since the additional electrons would partially fill higher lying, antibonding states. Exceptions may be Sm and Pu, which have eight valence electrons and could completely fill the 2g cluster state of e symmetry. Of those two, only Pu exists in a 4^+ oxidation state. In summary, our analysis points to the following elements as likely candidates for producing stable $\text{M}@C_{28}$ complexes: Mo , W , Ru , Os , Ce , Th , and Pu .

A recent calculation²⁰ for $\text{Ce}@C_{28}$ gives results that are consistent with our meta-atom model: the calculated binding energy of this system, 13.7 eV, is comparable to that of $\text{Zr}@C_{28}$ (12.6 eV¹⁰). In addition, covalent bonding was observed in this system between the Ce 4f states and the 2f levels of the cage.

An alternative application of our model is for predicting endohedral bonding in different fullerene cages, for example C_{32} . This cluster is similar in size and general character to C_{28} (see Table 1). One might therefore expect endohedral atoms which are very stable in C_{28} to be comparably stable in C_{32} . Our model, however, leads to very different predictions. C_{32} has four more

π electrons than C_{28} , which completely fill the 2f cluster levels (the ones available for creating bonds to the U 5f states, for example). This will greatly reduce the affinity between this cluster and U atoms. Evidence in support of this prediction already exists in the experiments of ref 8, which compare the relative abundances of fullerenes with and without endohedral atoms. Those experiments suggest that while the empty C_{28} and C_{32} fullerenes are of comparable stability, $U@C_{28}$ appears to be considerably more stable than $U@C_{32}$.

Finally, we turn to the bonding of endohedrals in C_{60} . $M@C_{60}$ complexes have relatively small binding energies of 1–2 eV, and bonding in these complexes is mostly ionic.^{21,22} This is in contrast to the strong, covalent bonding possible in $M@C_{28}$ as discussed above. The sheer size difference between the two fullerene cages is one reason for these differences in bonding. As shown in Table 1, the C_{60} shell has a radius of 6.61 au (about 3.5 Å). Even the largest endohedral atoms are too small to allow significant overlap between the endohedral orbitals and cluster orbitals in this case. On the other hand, even if the C_{60} fullerene cage were smaller in size, our model suggests that this cluster *could not* bond covalently to endohedral atoms located at the center of the cage since the HOMO of C_{60} has a character that corresponds to angular momentum $l = 5$ (h).¹⁸ The 2f states of C_{60} , which could bond to the 5f electrons of U, for example, lie on average about 3.5 eV below the HOMO and are completely full, making it unlikely that these levels could participate in covalent bonds with endohedral orbitals. It would be of interest to consider the implications of our meta-atom model to the bonding of small clusters inside C_{60} and larger fullerenes. Endohedral clusters could certainly be chosen to eliminate the size problem, and with proper choice of cluster pairs, the endohedral and cage wave functions could have matching character, leading to stable systems. The class of structures recently proposed by Zeger and Kaxiras²³ may fall in this category.

Discussion

Other models for endohedral bonding in fullerenes have been presented in the literature.^{21,22} For $M@C_{60}$ and larger systems, these models have been based essentially on charge transfer between the endohedral atom and the fullerene cage, and predictions for binding energies involve a comparison of ionization energy of the endohedral atom, the electron affinity of the cage, and the electrostatic interaction of a positively charged endohedral and negatively charged cage. We argued earlier that the extremely strong bonding in systems like $Zr@C_{28}$ cannot be explained by a simple ionic model. In fact, using the ionic model of ref²², for example, we find a maximum *ionic* bonding of about 4.5 eV in $Zr@C_{28}$, much less than the calculated 12.6 eV.

Recently, Guo et al.²⁴ have systematically studied $M@C_{28}$ complexes at the self-consistent-field Hartree–Fock (SCF HF) level of theory. These authors studied endohedrals from across the periodic table, computing equilibrium geometries and binding energies. In their analysis, they argue that thermodynamic stability of the endohedral complex is a key factor for formation of the $M@C_{28}$ systems. Addressing the general question of the formation of endohedral fullerenes of any size, they argue on empirical grounds that the electronegativity of the endohedral, coupled with its ionic radius, are the decisive factors. They suggest that successful endohedrals are those with an electronegativity of 1.54 or less.

The point of view taken in the present work is clearly different than that of ref²⁴. Rather than focusing on electronegativity, the meta-atom model attempts to address the factors directly involved in covalent bonding between the endohedral atom and small fullerene cages. On the basis of the results of our first-principles calculations,¹² we argue above that the angular momentum character of the endohedral atom valence states and of the cluster states near the Fermi level are the factors that determine relative

TABLE 2: Binding Energy ΔE for Various Endohedral Complexes $M@C_{28}$ Obtained by LDA and SCF HF (Ref 24) Calculations^a

endohedral complex	ΔE LDA (eV)	ΔE SCF HF (eV)
Si@ C_{28}	1.5	-7.8
Ge@ C_{28}	0.8	-6.3
Sn@ C_{28}	-0.9	-8.0
Ti@ C_{28}	9.8	-0.8
Zr@ C_{28}	12.9	2.8

^a The binding energies are referenced to the isolated atoms and C_{28} in their respective lowest energy spin states. The LDA results are for a symmetric, on-center endohedral atom, while the SCF HF values in general include a small, off-center relaxation of the endohedral atom. Negative values indicate that the isolated atom plus a bare C_{28} cage are more stable than the endohedral complex.

stability of the endohedral complexes C_{28} . Guo et al.²⁴ note two cases for which their electronegativity model fails to reproduce experiment. $Ti@C_{28}$ is a borderline case, as Ti has an electronegativity just over 1.54, yet $Ti@C_{28}$ is seen experimentally.⁸ The case of $Mg@C_{28}$ is more problematic. Mg has an electronegativity of 1.31 and an ionic radius of 0.78 Å, so that the electronegativity model clearly predicts that $Mg@C_{28}$ should be stable, yet this system has not been seen in experiments.⁸ The meta-atom model, by contrast, is consistent with experiment for both of these cases. In our model, Ti is expected to be strongly bound, in analogy to the isoelectronic $Zr@C_{28}$ and consistent with first-principles calculations.¹¹ Mg, on the other hand, with the valence electron configuration $3s^2$, should not bind effectively in C_{28} due to the depth of the cage 2s levels as discussed above for $Sn@C_{28}$ and should therefore not be seen experimentally.

It is interesting to compare the SCF HF binding energy results of ref²⁴ with those computed within the LDA. In Table 2 we compare results for systems that have been studied with both methods. The LDA binding energies are seen to be much larger than the SCF HF energies for every case. This reflects in part the tendency of the LDA to overbind molecules and that of SCF HF calculations to underbind. The following argument suggests that the LDA binding energies are more realistic: The experimental results on $U@C_{28}$ and $Zr@C_{28}$ ⁸ show that these endohedral complexes are produced in quantities comparable to C_{60} . Assuming that differences in formation kinetics are relatively small, these results suggest that C_{60} and $Zr@C_{28}$ should have similar thermodynamic stabilities. As seen in Table 1, the LDA predicts that C_{60} is more stable than bare C_{28} by about 0.5 eV/atom. If $Zr@C_{28}$ is to be comparable to C_{60} in stability, the binding energy for Zr in C_{28} must be of the order of 14 eV (producing an extra 0.5 eV binding energy/atom). This is indeed close to the predicted LDA value, but much larger than the corresponding SCF HF value of 2.8 eV. Note that the tendency of LDA to overbind molecules arises in computing the atomization energies; the relative energy comparisons made above do not reference free atoms and are thus expected to be a good estimates.

Summary

We have presented a simple model of endohedral bonding in small fullerene clusters. This model is based on a meta-atom view of the cluster in which principal and angular momentum quantum numbers are assigned¹⁸ to the cluster eigenstates. The character of the valence electron states near the Fermi level of the cluster determines the nature of bonding to endohedral atoms. We have illustrated the validity of the model by using it to explain the relative stability of $Sn@C_{28}$ and $Zr@C_{28}$, the first being a hypothetical structure that is not observed experimentally, while the second is a stable, experimentally produced structure. We have also used the model to understand the remarkable stability of the $U@C_{28}$ complex and to make specific predictions about the stability of other endohedral systems, including different elements and other fullerenes.

The authors would like to thank Dr. G. Stollhof for helpful suggestions regarding this work. K.J. gratefully acknowledges the support of the Research Corp. and a Research Professorship at Central Michigan University. E.K. acknowledges partial support from the Materials Research Laboratory of Harvard which is funded by the National Science Foundation. M.R.P. was supported in part by the Office of Naval Research.

References and Notes

- (1) Kroto, H. W.; Heath, J. R.; O'Brien, S. C.; Curl, R. F.; Smalley, R. E. *Nature* **1985**, *318*, 162.
- (2) Iijima, S. *Nature* **1991**, *354*, 56.
- (3) Pederson, M. R.; Broughton, J. Q. *Phys. Rev. Lett.* **1992**, *69*, 2689.
- (4) Ugarte, D. *Nature* **1992**, *356*, 776.
- (5) Heath, J. R., et al. *J. Am. Chem. Soc.* **1985**, *107*, 7779. Curl, R. F.; Smalley, R. E. *Science*, **1988**, *242*, 1017. Chai, Y., et al. *J. Phys. Chem.* **1991**, *95*, 7564; Weaver, J. H., et al. *Chem. Phys. Lett.* **1991**, *190*, 460.
- (6) Cioslowski, J.; Nanayakkara, A. *Phys. Rev. Lett.* **1992**, *69*, 2871.
- (7) Wang, Y.; Tomanek, D.; Ruoff, R. S. *Chem. Phys. Lett.* **1993**, *208*, 79.
- (8) Guo, T., et al. *Science* **1992**, *257*, 1661.
- (9) The structure of this cluster was first discussed by: Kroto, H. W. *Nature* **1987**, *329*, 529.
- (10) Pederson, M. R.; Laouini, N. *Phys. Rev. B* **1993**, *48*, 2733.
- (11) Dunlap, B. I.; Häberlen, O. D.; Rösch, N. *J. Phys. Chem.* **1992**, *96*, 9095. Häberlen, O. D.; Rösch, N.; Dunlap, B. I. *Chem. Phys. Lett.* **1992**, *200*, 418.
- (12) Jackson, K. A.; Kaxiras, E.; Pederson, M. R. *Phys. Rev. B* **1993**, *48*, 556.
- (13) Chang, A. H. H.; Zhao, K.; Ermler, W. C.; Pitzer, R. J. *Alloys Compounds*, in press.
- (14) Hohenberg, P.; Kohn, W. *Phys. Rev.* **1964**, *136*, B864. Kohn, W.; Sham, L. J. *Phys. Rev.* **1965**, *140*, A1133.
- (15) Pederson, M. R.; Jackson, K. A. *Phys. Rev. B* **1990**, *41*, 7453.
- (16) Jackson, K. A.; Pederson, M. R. *Phys. Rev. B* **1990**, *42*, 3276.
- (17) Pederson, M. R.; Jackson, K. A.; Boyer, L. L. *Phys. Rev. B* **1992**, *45*, 6919; Pederson, M. R.; Quong, A. A. *Phys. Rev. B* **1992**, *46*, 13584.
- (18) Haddon, R. C.; Brus, L. E.; Ragavachari, K. *Chem. Phys. Lett.* **1986**, *125*, 459; Fowler, P. W.; Woolrich, J. *Chem. Phys. Lett.* **1986**, *127*, 78. Ozaki, O.; Takahashi, A. *Chem. Phys. Lett.* **1986**, *127*, 242; Martins, J. L.; Troullier, N.; Weaver, J. H. *Chem. Phys. Lett.* **1992**, *180*, 457. Troullier, N.; Martins, J. L. *Phys. Rev. B* **1992**, *46*, 1754.
- (19) Cotton, R. F. *Chemical Applications of Group Theory*, 2nd ed.; Wiley-Interscience: New York, 1971.
- (20) Rösch, N.; Häberlen, O. D.; Dunlap, B. I. *Angew. Chem., Int. Ed. Engl.* **1993**, *32*, 108.
- (21) Cioslowski, J.; Raghavachari, K. *J. Chem. Phys.* **1993**, *98*, 8734. Cioslowski, J.; Fleischmann, E. D. *J. Chem. Phys.* **1991**, *94*, 3730. Cioslowski, J. *J. Am. Chem. Soc.* **1991**, *113*, 4139. Wang, Y.; Tomanek, D.; Ruoff, R. S. *Chem. Phys. Lett.* **1993**, *208*, 79.
- (22) Erwin, S. C. In *Buckminsterfullerenes*; Billups, W. E.; Ciofolini, M. A., Eds.; VCH: New York, 1993.
- (23) Zeger, L.; Kaxiras, E. *Phys. Rev. Lett.* **1993**, *70*, 2920.
- (24) Guo, T.; Smalley, R. E.; Scuseria, G. E. *J. Chem. Phys.* **1993**, *99*, 352.